Available online at www.sciencedirect.com
ScienceDirect
Tectonophysics 428 (2006) 87–94
TECTONOPHYSICS
www.elsevier.com/locate/tecto

Increasing critical sensitivity of the Load/Unload Response Ratio before large earthquakes with identified stress accumulation pattern

Huai-zhong Yu [a,*], Zheng-kang Shen [a,b], Yong-ge Wan [a], Qing-yong Zhu [c], Xiang-chu Yin [d]

[a] State Key Laboratory of Earthquake Dynamics, Institute of Geology, China Earthquake Administration, Beijing 100029, China
[b] Department of Earth and Space Sciences, University of California, Los Angeles, CA 90095-1567, USA
[c] School of Mathematics and Computational Science, Zhongshan University, Guangzhou 510275, China
[d] State Key Laboratory of Nonlinear Mechanics, Institute of Mechanics, Chinese Academy of Sciences, Beijing 100080, China

Received 4 October 2005; received in revised form 17 September 2006; accepted 21 September 2006
Available online 9 November 2006

Abstract

The Load/Unload Response Ratio (LURR) method is proposed for short-to-intermediate-term earthquake prediction [Yin, X.C., Chen, X.Z., Song, Z.P., Yin, C., 1995. A New Approach to Earthquake Prediction — The Load/Unload Response Ratio (LURR) Theory, Pure Appl. Geophys., 145, 701–715]. This method is based on measuring the ratio between Benioff strains released during the time periods of loading and unloading, corresponding to the Coulomb Failure Stress change induced by Earth tides on optimally oriented faults. According to the method, the LURR time series usually climb to an anomalously high peak prior to occurrence of a large earthquake. Previous studies have indicated that the size of critical seismogenic region selected for LURR measurements has great influence on the evaluation of LURR. In this study, we replace the circular region usually adopted in LURR practice with an area within which the tectonic stress change would mostly affect the Coulomb stress on a potential seismogenic fault of a future event. The Coulomb stress change before a hypothetical earthquake is calculated based on a simple back-slip dislocation model of the event. This new algorithm, by combining the LURR method with our choice of identified area with increased Coulomb stress, is devised to improve the sensitivity of LURR to measure criticality of stress accumulation before a large earthquake. Retrospective tests of this algorithm on four large earthquakes occurred in California over the last two decades show remarkable enhancement of the LURR precursory anomalies. For some strong events of lesser magnitudes occurred in the same neighborhoods and during the same time periods, significant anomalies are found if circular areas are used, and are not found if increased Coulomb stress areas are used for LURR data selection. The unique feature of this algorithm may provide stronger constraints on forecasts of the size and location of future large events.

Keywords: Load/Unload Response Ratio; Coulomb stress; Critical region of precursory LURR anomaly; Earthquake prediction

1. Introduction

Over the past decade an earthquake prediction method named the Load/Unload Response Ratio (LURR) has been developed by Yin and others (e.g. Yin et al., 1995, 2000, 2004). Before the occurrence of a large earthquake ($M>6.0$), anomalous increase in the time series of LURR

* Corresponding author. State Key Laboratory of Earthquake Dynamics, Institute of Geology, China Earthquake Administration, P.O. Box 9803, Beijing 100029, China. Tel.: +86 10 62009146.
E-mail addresses: yuhz@lnm.imech.ac.cn (H. Yu), zshen@ess.ucla.edu (Z. Shen), mcszqy@mail.sysu.edu.cn (Q. Zhu), xcyin@public.bta.net.cn (X. Yin).

0040-1951/$ - see front matter © 2006 Elsevier B.V. All rights reserved.
doi:10.1016/j.tecto.2006.09.006

within a time frame from months to years, has often been observed (Yin et al., 1995, 2000; Zhang et al., 2004). This phenomenon can be used as an important precursor to predict large earthquakes. The evolution of LURR time series is believed to reflect the damage evolution of a brittle heterogeneous system. When the system is stable, the ways it responses to loading and unloading are nearly the same, whereas when the system is in an unstable state, the responses usually become quite different. In earthquake prediction practices, application of the LURR method typically involves calculating the Earth tide induced Coulomb failure stress change (ΔCFS) on faults, differentiating its loading and unloading periods, evaluating the Benioff strain releases of earthquakes during both periods, and calculating the ratio between the two Benioff strain releases. In retrospective studies, the LURR method has been applied in numerous short-to-intermediate-term earthquake prediction practices, in which anomalously high LURR values have often been detected months to years before large earthquakes (Yin et al., 2000; Zhang et al., 2004).

The static (Coulomb) stress interaction between earthquakes is another important discovery obtained from analyzing seismic activity patterns in recent years (e.g. Harris and Simpson, 1996; Harris, 1998). To investigate such an interaction, a technique to compute earthquake induced Coulomb stress change using the elastic-dislocation method was applied to examine the temporal and spatial seismic activity pattern (e.g. Stein et al., 1994; King and Cocco, 2001). Previous investigations have indicated that the change of seismic activity often corresponds to the Coulomb stress change. For instance, by analyzing the change of the Coulomb stress field from historic coseismic ruptures in southern California, Deng and Sykes (1997) found that more than 85% of the earthquakes with magnitudes $M>5.0$, and more than 95% of the earthquakes with magnitudes $M>6.0$ occurred in the regions with increased Coulomb stress between 1812 and 1995. Stein (1999) also found that most earthquakes occurred in the regions of Coulomb stress increase when they investigated the pattern of Coulomb stress change in the vicinity of the Anatolian fault, Turkey, between 1939 and 1992. Similar results were obtained by Nalbant et al. (1998) when they studied stress triggering of 29 earthquakes in Turkey and northern Aegean Sea. Papadimitriou and Sykes (2001) further concluded that all the earthquakes of $M>6.5$ that occurred in the northern Aegean Sea during the 20th century fell in the regions with increased Coulomb stress. These results indicate that evaluation of the Coulomb stress change can be an important tool to assess the potential of occurrence of large earthquakes (Toda et al., 1998; Troise et al., 1998; Fox and Dziak, 1999; Hubert-Ferrari et al., 2000; Wan et al., 2004).

In this paper, we experiment a revised approach to assess earthquake potential by replacing the previously used circular critical region with an area where there are noticeable increases of Coulomb stress for the LURR estimation within a given time frame before an earthquake. To show the validity of the approach, the 1989 Mw 6.9 Loma Prieta, 1992 Mw 7.3 Landers, 1994 Mw 6.7 Northridge, and 1999 Mw 7.1 Hector Mine earthquakes in California are chosen as the examples.

2. The LURR method and its computation

The LURR values that measure the degree of closeness to instability for a nonlinear system can be defined as

$$Y = \frac{X_+}{X_-}, \tag{1}$$

where "+" and "−" refer to the loading and unloading processes, and X is the response rate (Yin et al., 1995, 2000). Suppose that P and R are respectively the load and response of the nonlinear system, then

$$X = \lim_{\Delta P \to 0} \frac{\Delta R}{\Delta P}, \tag{2}$$

can be defined as the response rate, where ΔR denotes the small increment of R, resulted from a small change of ΔP on P.

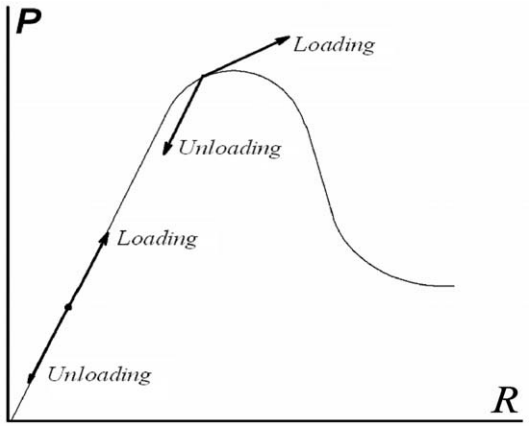

Fig. 1. Schematic view of the constitutive law of a brittle mechanic system. P and R correspond to the load and response of a mechanic system. The response is linear to the load and unload when the load is well below the strength of the system, and becomes nonlinear when the system is close to failure.

When the system is in a stable state, $x_+ \approx x_-$ and LURR ≈ 1. When the system evolves beyond the linear state, usually $x_+ > x_-$, and LURR > 1 (Fig. 1). Thus, the LURR can be used as a criterion to judge the state of stability for a system before its macro-failure.

In earthquake prediction practice using the LURR method, the seismic energy release within certain temporal and spatial windows is usually used as data input. Loading and unloading periods are determined by calculating the earth tide induced ΔCFS along a tectonically favored rupture direction on a specified fault plane: when ΔCFS > 0, it is in a loading state; and when ΔCFS < 0, it is in an unloading state. The LURR is thus expressed as a ratio between energy released during loading and that released during unloading periods. Specifically,

$$Y_m = \frac{(\sum_{i=1}^{N+} E_i^m)_+}{(\sum_{i=1}^{N-} E_i^m)_-}, \quad (3)$$

where E_i is seismic energy released by the i-th event, and $m = 0$, 1/3, 1/2, 2/3, or 1. When $m = 1/2$, E^m denotes the Benioff strain; if $m = 1/3$ and 2/3, E^m represents the radius and area scales of the focal zone; and in the case where $m = 0$, E^m equals to N^+ or N^-, denoting the numbers of events that occurred during the loading and unloading stages, respectively. To avoid violent fluctuations due to poor statistics, the loading and unloading periods are usually summed over many load–unload cycles within the temporal window. The spatial window for LURR evaluation is determined by computing the LURR anomaly within differently sized regions centered at the epicenter of the oncoming large event to reach the maximum LURR precursory anomaly (Yin et al., 2002).

2.1. Assessment of regions with higher pre-seismic stress

Yin et al. (2002) found that size designation of the critical seismogenic region (considered as the spatial window in LURR practices) prior to an earthquake has great influence on the predictive power of the LURR method. In order to optimally determine the regions which demonstrate anomalous changes of the LURR time series before an earthquake, we attempt an approach focusing on the specific area with increased Coulomb stress before the event. There have been many investigations about the distribution of Coulomb stress change before an earthquake (e.g. Harris and Simpson, 1992; Stein et al., 1992, 1994, 1997; Deng and Sykes, 1997). One approach to determine the regions with higher pre-seismic stress is to approximate stress evolution resulted from past earthquakes and tectonic loading (Nalbant et al., 1998; Hubert-Ferrari et al., 2000). King and Cocco (2001) pointed out that prior to the 1992 Landers earthquake, much of the Coulomb stress increase within 50 km of the epicenter was caused by four prior earthquakes of $M > 5$ from 1975 to 1992. Together these earthquakes created a narrow zone with 0.7–1.0 bar of the Coulomb stress increase. In spite of the well-determined spatial pattern of Coulomb stress change that resulted from the previous large earthquakes, this method, however, offers little information about the short-to-intermediate-term variation of the Coulomb stress field, making it difficult to assess the short-to-intermediate-term earthquake potential.

In this paper, we attempt to revise the LURR method by optimally locating the region within which the LURR is evaluated; i.e. we select the region within which the Coulomb stress change is likely to bring the seismogenic fault of the future earthquake closer to failure. This is done by bringing the fault back to its stress state before it was relaxed through the earthquake. The physical basis of this back-slip model was developed by Savage (1983). Bowman and King (2001) applied the model, combining with assessing preseismic acceleration of seismicity, to examine the $M \geq 6.5$ earthquakes in California from 1950 to 2000. They proposed that the effectiveness for seismic hazard evaluation could be enhanced by substituting the circular critical region with the areas of increased Coulomb stress. In addition, Sammis et al. (2004) and Levin et al. (2006) also linked this stress recovery method to the evolution of seismicity before large earthquakes. Our approach basically follows these works in this regard. For a single fault patch model, during the establishment of the criticality, the tectonic stress must be accumulated not only at the fault surface but also in a region surrounding the fault. The stress field is usually not uniform in the region due to heterogeneity of the crustal media and stress release of previous large events. Some parts of the region may be accumulated with higher stresses than the other parts. The stress distribution, particularly where the relatively higher stresses are situated with respect to the seismogenic fault, could manifest the epicentral location of the subsequent earthquake. Then, during the dynamic rupture of the earthquake, the parts of the region with higher tectonic stress might become relaxed the most and were removed away from the critical state. Hence, it is perhaps reasonable to assume (as Bowman and King (2001) did in their seismicity and stress accumulation analysis before large earthquakes) that the parts of the region where the Coulomb stress is relaxed the most during an earthquake are also the parts of the region which were

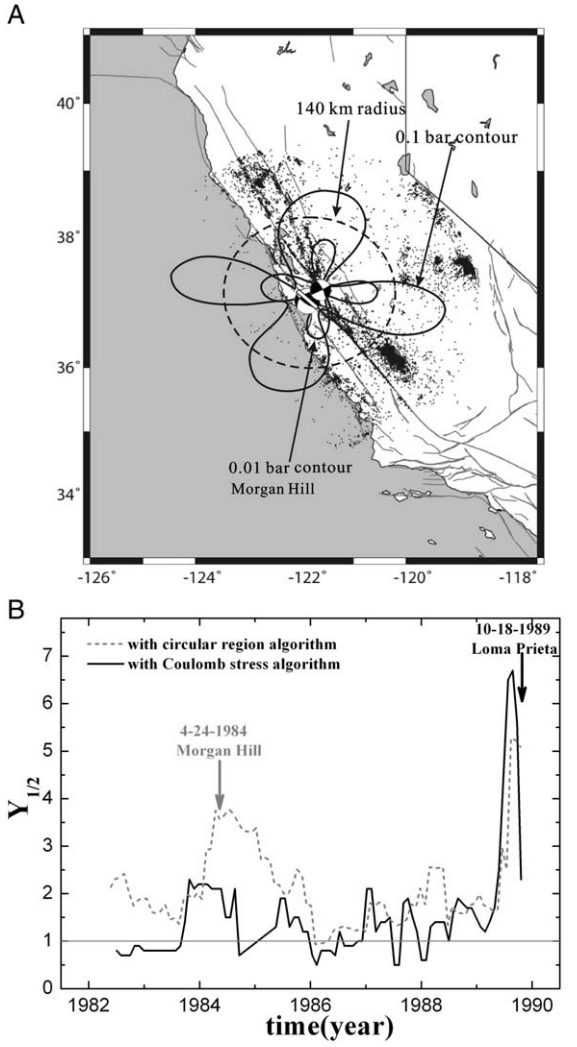

Fig. 2. (A) Earthquake data selection regions for the Coulomb stress algorithm and the circular region algorithm before the Loma Prieta earthquake. The solid curve delineates the regions adopted by the Coulomb stress algorithm with increased Coulomb stress of >0.1 bar, and the dashed circle shows a region adopted by the circular region algorithm of 140 km radius centered at the epicenter of the Loma Prieta earthquake. Dots represent the earthquakes falling in a circular region of 270 km radius from 1-1-1981 to 10-17-1989. Two focal mechanisms, one big and one small, denote respectively the 1989 Loma Prieta and 1984 Morgan Hill earthquakes. The contour of increased pre-seismic Coulomb stress of >0.01 bar for the Morgan Hill earthquake is also shown. (B). Time series of LURR for the Coulomb stress algorithm (solid curve) and the circular region algorithm (gray dashed curve) before the Loma Prieta earthquake with the critical regions as defined in (A), in which the Benioff strain was computed as the loading/unloading response. Specific parameters for LURR evaluation are: Strike=123°, Dip=71°, Rake=128°, and Depth=15 km (Harvard CMT solution).

pre-stressed the most before the event. To reproduce the pattern of stress change and identify the areas with higher pre-stress field before an earthquake where anomalous change of LURR is expected, we impose the coseismic slip (either hypothetical or known for a retrospective study) backward along the seismogenic fault in a continuum media using a dislocation code developed by Okada (1992).

2.2. Application to seismic data

As a retrospective study, we apply our method to the Coulomb stress change and the change of LURR time series associated with the Mw≥6.7 earthquakes in

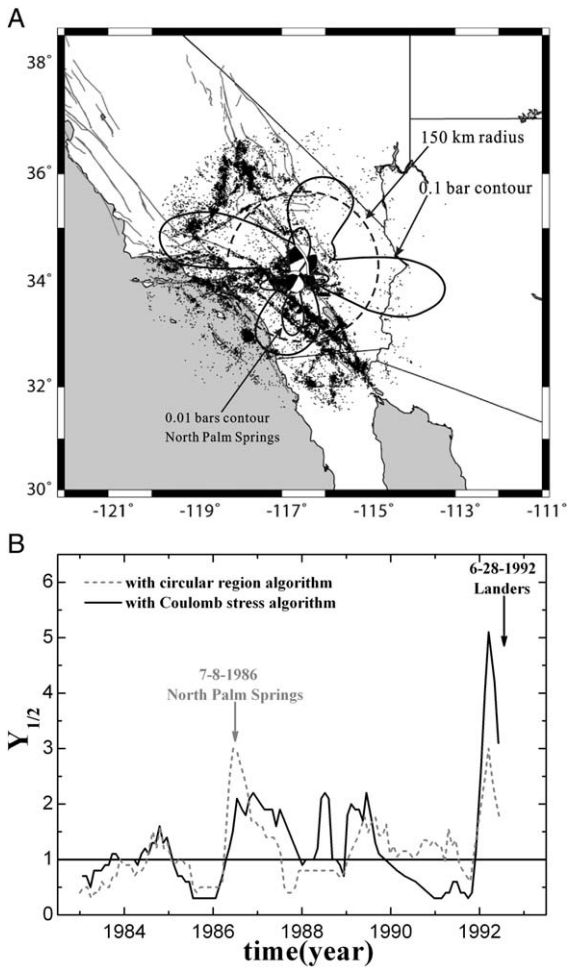

Fig. 3. Data selection regions (A) and LURR time series (B) before the Landers earthquake. All the descriptions are the same as for Fig. 2 except some specific parameters used: circular region radius: 150 km; earthquake catalog coverage, 320 km radius centered at the Landers epicenter and time period between 1-1-1982 and 6-27-1992; two focal mechanisms are for the 1992 Landers and 1986 North Palm Springs earthquakes. The Coulomb stress contour of >0.01 bar is for the North Palm Springs earthquake. Parameters for LURR evaluation are: Strike=341°, Dip=70°, Rake=−172°, and Depth=15 km (Harvard CMT solution).

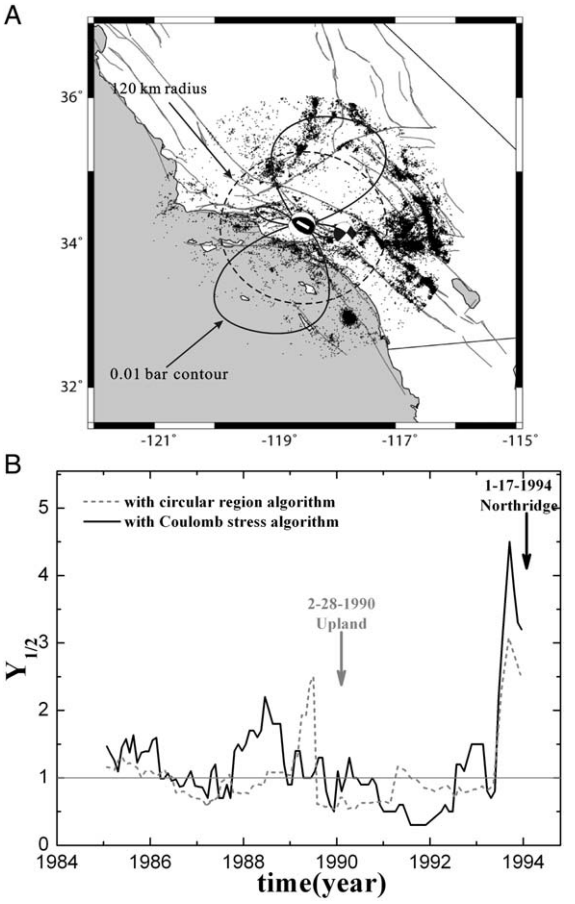

Fig. 4. Data selection regions (A) and LURR time series (B) before the Northridge earthquake. All the descriptions are the same as Fig. 2 except some specific parameters used: Coulomb stress contour, 0.01 bar; circular region radius: 120 km; earthquake catalog coverage, 210 km radius centered at the Northridge epicenter and time period between 1-1-1984 and 1-16-1994; two focal mechanisms are for the 1994 Northridge and 1990 Upland earthquakes. Parameters for LURR evaluation are: Strike=278°, Dip=42°, Rake=65°, and Depth=15 km (Harvard CMT solution).

California over last 20 years (i.e. the 1989 Mw 6.9 Loma Prieta, 1992 Mw 7.3 Landers, 1994 Mw 6.7 Northridge, and 1999 Mw 7.1 Hector Mine earthquakes). The regions of Coulomb stress increase before these earthquakes are computed using the technique of backward slipping above. Detailed source models and slip distributions were adopted from Reasenberg and Simpson (1992), Hudnut et al. (1994), Wald et al. (1996), and Hauksson et al. (2002) for the four quakes respectively. In this study, small to moderate sized earthquakes (their catalog retrieved from the ANSS websites http://www.ncedc.org/anss/) of $1.5<M<5.5$ within the Coulomb stress increase regions were used to compute the LURR time series. Note that the focal mechanisms of these small earthquakes are assumed in agreement with that of the main shock to contribute positively to ΔCFS for the main shock. This assumption is supported by studies of Hauksson (1994), Hauksson et al. (2002), and Hardebeck and Hauksson (2001), which demonstrated that the focal mechanisms of regional small earthquakes prior to the Landers and Hector Mine earthquakes were quite consistent with that of the ensuing main shocks. In our study, the internal friction coefficient we adopted to calculate ΔCFS is 0.4. The method for definition of the optimal critical region size of precursory LURR

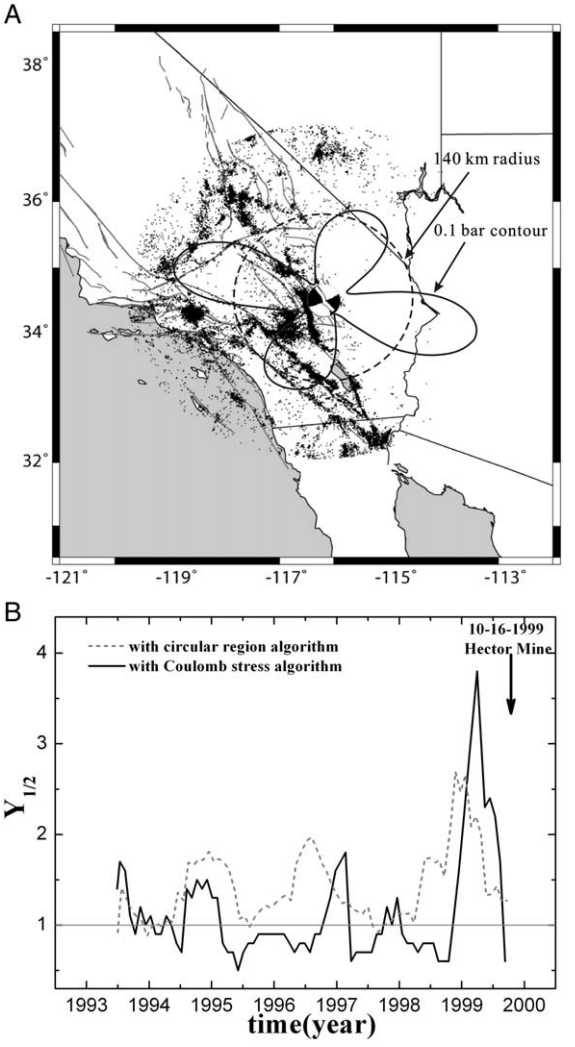

Fig. 5. Data selection regions (A) and LURR time series (B) before the Hector Mine earthquake. All the descriptions are the same as Fig. 2 except some specific parameters used: circular region radius: 140 km; earthquake catalog coverage, 300 km radius centered at the Hector Mine epicenter and time period between 7-1-1992 and 10-15-1999. Parameters for LURR evaluation are: Strike=336°, Dip=80°, Rake=174°, and Depth=15 km (Harvard CMT solution).

anomaly is similar to the methodology given by Yin et al. (2002). The major difference lies in that the region is not decided by changing the size of a circular region, but by determining the range of Coulomb stress values set by the ensuing large event. At each stress value, the Benioff strain release ($m=1/2$ in Eq. (3)) of earthquakes within the stress contour were used to calculate the LURR time series, and the critically stressed region is then defined as the Coulomb stress contour that maximizes the LURR anomaly prior to the event.

The optimal critical regions of precursory LURR anomaly for the four events are shown in Figs. 2A, 3, 4 and 5A, delineated by the Coulomb stress contours of 0.1, 0.1, 0.01, and 0.1 bars. Stress change of 0.1 bar is also believed to be the minimum value to have effects on triggering of post-seismic seismicity (Hardebeck et al., 1998; Anderson and Johnson, 1999; King and Cocco, 2001). Smaller threshold (0.01 bar) is attributed to the Coulomb stress contour for the Northridge earthquake, which is the event whose magnitude is significantly less than the other three and might have the triggering effect somewhat different from the others. The earthquakes occurred within 270, 320, 210, and 300 km distance from the epicenters and 7.5–10 years prior to the main shocks are displayed. Also shown in the figures are the circular critical regions with their radii of 140, 150, 120, and 140 km for the four events respectively. These circular regions, despite of shape difference, are about the same in areal size as the regions delineated by the Coulomb stress contours mentioned above. Figs. 2B, 3, 4 and 5B show the evolution of LURR time series computed using earthquakes within both the Coulomb stress increased and the circular areas, with a temporal window of 1 year at a sliding step of 1 month.

3. Comparison and discussion

Comparing the LURR time series derived using the Coulomb stress contour and circular region as data selection criteria, it is clear that both algorithms have yielded significant anomalies prior to the ensuing major events. The LURR time series of both algorithms are at a low level for most of the time, and reach the maxima a few months before the quakes. These results are consistent with previous studies by Yin et al. (2000, 2002), which indicated that the LURR values were between 0 and 2.2 for several years until several months before the quake when, the LURR values peaked at a high value (~ 7, 5, 5, and 4 for the four events), and then began to drop 1, 1, 2, and 4 months before the event. More detailed comparison between the results obtained using the Coulomb stress and circular region data selection algorithms, however, does show some noticeable differences. They are:

1. Although the LURR anomalies produced by the two algorithms before major events appear at about the same time, the ones produced by the Coulomb stress algorithm look more prominent than the others produced by the circular region algorithm. The corresponding LURR peak values are 6.8 vs. 5.3, 5.2 vs. 3.3, 4.5 vs. 3.1, and 3.8 vs. 2.7 for the Loma Prieta, Landers, Northridge, and Hector Mine earthquakes respectively (Figs. 2B, 3, 4 and 5B). Such contrasts make the anomalies stand out more clearly in the entire time series, and would represent less ambiguous warning signals for future events.
2. The Coulomb stress algorithm seems to be more sensitive to detect future earthquakes of particular magnitude range and location than the circular region algorithm. All the LURR time series produced by the Coulomb stress algorithm remain at a relatively low level (<2.5) for the entire time periods until a few months before the ensuing events, when they start to climb to remarkable peaks (Figs. 2B, 3, 4 and 5B). On the other hand, multiple maxima appear in the LURR time series produced by the circular region algorithm, most of which correspond to the incoming regional earthquakes of moderate to large sizes to occur inside the circular regions, not unique just to the large events occurred at the centers of the circles. For example, the LURR time series peaked right before the 24 April 1984 M6.2 Morgan Hill and 8 July 1986 M6.0 North Palm Springs earthquakes (Figs. 2 and 3). It also peaked 7 months before the 28 February 1990 M5.7 Upland earthquake (Fig. 4). There was no peak of >2.0 in the LURR time series 1993.5–1999.0 in the Hector Mine region, which is consistent with the regional seismicity pattern during this time period (Fig. 5).

The LURR is computed in terms of the tidal stress triggering of earthquakes. Tidal stress is several orders of magnitude smaller than the tectonic stress, it could only trigger, not engender, earthquakes by itself. When the tectonic stress is low, it is difficult for tidal stress to trigger any earthquakes, so that the LURR must be low. When the tectonic stress is at a high level, the source media may be sensitive to a small extrinsic disturbance, and earthquakes could easily be triggered by increased Coulomb stress induced by the tidal stress (Cochran et al., 2004; Tanaka et al., 2004), so that the LURR might also be anomalously increased. For a given located fault patch, if the part of its surrounding regions, which manifests its stress state relatively more effectively, is loaded with anomalously

high Coulomb stress, it would tend to be driven toward failure.

The earthquakes we show above are possibly such examples, whose high Coulomb stress in its surrounding region is detected by the anomalously high sensitivity of seismic strain release to cyclical tidal loading (LURR) prior to the event. We note that the areas of increased sensitivity to cyclical stress variations have also been proposed to be areas of accelerating seismicity (Sykes and Jaume, 1990; Bufe and Varnes, 1993; Bowman and King, 2001; Sammis et al., 2004; Levin et al., 2006). While both approaches might provide information about the approaching criticality of the system, we believe that our algorithm could be tuned toward detecting some specific events. The test regions of this study are specifically tailored for testing events of specific magnitudes centered at the seismogenic faults, earthquakes occurred within a circular region but off the Coulomb stress increase area (where the stress change may be less effective in manifesting the Coulomb stress change on the fault patch), are excluded from the evaluation of LURR (such as the regions southeast of the Loma Prieta epicenter along the San Andreas fault in Fig. 2A, near the northern San Jacinto fault in Fig. 3A, and east of the Northridge epicenter in Fig. 4A), the sensitivity of the LURR method could therefore be enhanced. On the other hand, for the circular region algorithm, because of its uniform selection of the region for LURR testing, it is less sensitive to a scenario earthquake; instead, it could be used for detecting the potential of a wider range of earthquakes, with less sensitivity. Hence, rather than the circular seismogenic regions, the Coulomb stress increase regions with anomalously increased LURR values before a large earthquake could provide a relatively more precise estimation of the criticality of the ensuing event. Knowing this unique characteristic of the Coulomb stress approach, we might use that for testing various kinds of scenario earthquakes in the future.

4. Conclusion

We find that by combining the LURR method with the evaluation of Coulomb stress increase before an earthquake, the predictive power of current LURR technique can be improved. At present time it is still difficult to apply the approach to practical real-time prediction of earthquakes because it is hard to pre-determine the epicentral location and extent of the fault rupture prior to a future earthquake. However, the approach presented in this paper allows us to systematically search for the locations of future scenario earthquakes, if seismogenic fault geometries and regional tectonic stress setting are known. And, even if such a priori information is not available, one could still presume all the possible earthquake scenarios including the location, magnitude, and mechanism and apply the approach to evaluate the corresponding LURR. Analysis of the anomalies in the LURR time series may provide us with seismic potential evaluation with estimates of all the crucial parameters provided such as earthquake location, time, magnitude, and mechanism.

Acknowledgement

We are grateful to the careful reviews made by the editor and two anonymous reviewers. We also thank Roland Burgmann and Yuhua Zeng for their constructive comments and suggestions. The research was supported by the Joint Earthquake Science Foundation of China (Grant nos. 606018, 104128), China Postdoctoral Science Foundation (Grant no. 2005037384), the National Natural Science Foundation of China (Grant nos. 40334042, 10572154, 40374012), and the Ministry Of Science and Technology of China (Grant Nos. 2002CCA04500, 2004CB418403).

References

Anderson, G., Johnson, H., 1999. A new statistical test for static stress triggering: application to the 1987 Superstition Hills earthquake sequence. J. Geophys. Res. 104, 20,153–20,168.

Bowman, D.D., King, G.C.P., 2001. Accelerating seismicity and stress accumulation before large earthquake. Geophys. Res. Lett. 28 (21), 4039–4042.

Bufe, C.G., Varnes, D.J., 1993. Predictive modeling of the seismic cycle of the greater San Francisco Bay region. J. Geophys. Res. 98 (B6), 9871–9883.

Cochran, E.S., Vidale, J.E., Tanaka, S., 2004. Earthquake tides can trigger shallow thrust fault earthquakes. Science 306, 1164–1166.

Deng, J., Sykes, L.R., 1997. Evolution of stress field in southern California and triggering of moderate-size earthquakes: a 200 years prospective. J. Geophys. Res. 102, 9859–9886.

Fox, C.G., Dziak, R.P., 1999. Internal deformation of the Gorda Plate observed by hydroacoustic monitoring. J. Geophys. Res. 104, 17603–17615.

Hardebeck, J.L., Hauksson, E., 2001. Crustal stress field in southern California and its implications for fault mechanics. J. Geophys. Res. 106, 21859–21882.

Hardebeck, J.L., Nazareth, J.J., Hauksson, E.J., 1998. The static stress change triggering model: constraints from two southern California aftershock sequences. J. Geophys. Res. 103, 24, 427–24, 437.

Harris, R.A., 1998. Earthquake stress trigger, stress shadows, and seismic hazard. J. Geophys. Res. 103, 24,347–34,358.

Harris, R.A., Simpson, R.W., 1992. Changes in static stress on southern California faults after the 1992 Landers earthquake. Nature 360, 251–254.

Harris, R.A., Simpson, R.W., 1996. In the shadow of 1957 — the effect of the great Ft. Tejon earthquake on subsequent earthquakes in southern California. Geophys. Res. Lett. 23, 229–232.

Hauksson, E., 1994. State of stress from focal mechanisms before and after the 1992 Landers earthquake sequence. Bull. Seismol. Soc. Am. 84 (3), 917–934.

Hauksson, E.L., Jones, M., Hutton, K., 2002. The 1999 Mw 7.1 Hector Mine, California, earthquake sequence: complex conjugate strike-slip faulting. Bull. Seismol. Soc. Am. 92, 1154–1170.

Hubert-Ferrari, A., Barka, A., Jacques, E., Nalbant, S., Meyer, B., Armijo, R., Tapponnier, P., King, G.C.P., 2000. Seismic hazard in the Marmara Sea region following the 17 August 1999 Izmit earthquake. Nature 404, 269–273.

Hudnut, K.W., Bock, Y., Cline, M., Fang, P., Freymueller, J., Gross, K., Jackson, D., Larson, S., Lisowski, M., Shen, Z., Svarc, J., 1994. Coseismic displacements in the Landers sequence. Bull. Seismol. Soc. Am. 84, 625–645.

King, G.C.P., Cocco, M., 2001. Fault interaction by elastic stress changes: new clues from earthquake sequences. Adv. Geophys. 44, 1–38.

Levin, S.Z., Sammis, C.G., Bowman, D.D., 2006. An observational test of the stress accumulation model based on seismicity preceding the 1992 Landers, CA earthquake. Tectonophysics 413, 39–52.

Nalbant, S.S., Hubert–Ferrari, A., King, G.C.P., 1998. Stress coupling between earthquakes in northwest Turkey and the north Aegean Sea. J. Geophys. Res. 103, 24, 469–24, 486.

Okada, Y., 1992. Internal deformation due to shear and tensile faults in a half–space. Bull. Seismol. Soc. Am. 82, 1018–1042.

Papadimitrious, E.E., Sykes, L.R., 2001. Evolution of the stress field in the northern Aegean sea. Geophys. J. Int. 146, 747–759.

Reasenberg, P.A., Simpson, R.W., 1992. Response of regional seismicity to the static stress change produced by the Loma Prieta earthquake. Science 255, 1687–1690.

Sammis, C.G., Bowman, D.D., King, G.C.P., 2004. Anomalous seismicity and accelerating moment release preceding the 2001 and 2002 earthquakes in northern Baja California, Mexico. Pure Appl. Geophys. 161, 2369–2378.

Savage, J.C., 1983. A dislocation model of strain accumulation and release at a subduction zone. J. Geophys. Res. 88, 4948–4996.

Stein, R.S., 1999. The role of stress transfer in earthquake occurrence. Nature 402, 605–609.

Stein, R.S., King, G.C.P., Lin, J., 1992. Change in failure stress on the southern San Andreas fault system caused by the 1992 Magnitude=7.4 Landers earthquake. Science 258, 1328–1332.

Stein, R.S., King, G.C.P., Lin, J., 1994. Stress triggering of the 1994 M=6.7 Northridge, California, earthquake by its predecessors. Science 265, 1432–1435.

Stein, R.S., Barka, A.A., Dieterich, J.H., 1997. Progressive failure on the North Anatolian fault since 1939 by earthquake stress triggering. Geophys. J. Int. 128, 594–604.

Sykes, L.R., Jaume, S., 1990. Seismic activity on neighboring faults as a long-term precursor to large earthquakes in the San Francisco Bay Area. Nature 348, 595–599.

Tanaka, S., Ohtake, M., Sato, H., 2004. Tidal triggering of earthquakes in Japan related to the regional tectonic stress. Earth Planets Space 56, 511–515.

Toda, S., Stein, R.S., Reasenberg, P.A., Dieterich, J.H., 1998. Stress transferred by the Mw=6.5 Kobe, Japan, shock: effect on aftershocks and future earthquake probabilities. J. Geophys. Res. 103, 24,543–24,565.

Troise, C., De Natale, G., Pingue, F., Petrazzuoli, S.M., 1998. Evidences for static stress interaction among earthquakes in the South–Central Apennines (Italy). Geophys. J. Int. 134, 809–817.

Wald, D.J., Heaton, T.H., Hudnut, T.W., 1996. The slip history of the 1994 Northridge, California, earthquake determined from strong ground motion, teleseismic, GPS, and leveling data. Bull. Seismol. Soc. Am. 86, S49–S70.

Wan, Y.G., Wu, Z.L., Zhou, G.W., 2004. Focal mechanism dependence of static stress triggering of earthquakes. Tectonophysics 390, 235–243.

Yin, X.C., Chen, X.Z., Song, Z.P., Yin, C., 1995. A new approach to earthquake prediction — the Load/Unload Response Ratio (LURR) theory. Pure Appl. Geophys. 145, 701–715.

Yin, X.C., Wang, Y.C., Peng, K., Bai, Y.L., Wang, H., Yin, X.F., 2000. Development of a new approach to earthquake prediction: Load/Unload Response Ratio (LURR) theory. Pure Appl. Geophys. 157, 2365–2383.

Yin, X.C., Mora, P., Peng, K.Y., Wang, Y.C., Weatherly, D., 2002. Load–Unload Response Ratio and Accelerating Moment/Energy Release, Critical Region Scaling and earthquake prediction. Pure Appl. Geophys. 159, 2511–2524.

Yin, X.C., Yu, H.Z., Kukshenko, V., Xu, Z.Y., Wu, Z.S., Li, M., Peng, K.Y., Elizarov, S., Li, Q., 2004. Load–Unload Response Ratio (LURR), Accelerating Moment/Energy Release (AM/ER) and State Vector evolution as precursors to failure of rock specimens. Pure Appl. Geophys. 161, 2405–2416.

Zhang, Y.X., Yin, X.C., Peng, K.Y., 2004. Spatial and temporal variation of LURR and its implication for the tendency of earthquake occurrence in Southern California. Pure Appl. Geophys. 161, 2359–2367.